Solid State Communications 149 (2009) 1888–1893

Contents lists available at ScienceDirect

Solid State Communications

journal homepage: www.elsevier.com/locate/ssc

Optical properties of a superconducting annular periodic multilayer structure

Mei-Soong Chen [a], Chien-Jang Wu [b,*], Tzong-Jer Yang [c,*]

[a] Department of Electrophysics, National Chiao-Tung University, Hsinchu 300, Taiwan

[b] Institute of Electro-Optical Science and Technology, National Taiwan Normal University, Taipei 116, Taiwan

[c] Department of Electrical Engineering, Chung Hua University, Hsinchu 300, Taiwan

ARTICLE INFO

Article history:
Received 30 May 2009
Accepted 2 August 2009 by Y.E. Lozovik
Available online 6 August 2009

PACS:
41.20.JB
42.70.Qs
74.20.De
74.25.Gz

Keywords:
A. Superconductors
A. Thin films
D. Optical properties

ABSTRACT

The optical properties of a superconducting annular Bragg reflector (SABR) are theoretically investigated based on the transfer matrix method for the cylindrical waves. For TM wave at an azimuthal mode number, $m \geq 1$, it is found that there exist some novelties compared with the usual superconducting planar Bragg reflector (SPBR). An additional high-reflectance band is seen and some reflection dips near the threshold wavelength of a superconductor are generated as well. These two special results arising from the higher order azimuthal mode of the cylindrical waves are not found in the SPBR. The results suggest that the SABR could be used to design a narrowband transmission filter or an annular resonator without introducing any physical defect layer in the structure.

1. Introduction

The study of a Bragg reflector (BR) or one-dimensional photonic crystal (1DPC) is an interesting subject and has attracted a lot of attention in recent years. There have been many reports on the calculations of the photonic band structures in 1DPCs so far [1–3]. It is known that PCs have photonic band gaps (PBGs) at which the electromagnetic waves cannot propagate through the layered structures. Materials with PBGs play an important role in modern photonic science and technology.

In the earlier stage, the PBG structures were mainly fabricated by using the usual dielectrics, semiconductors and metals as well. Recently, the studies of the photonic band structures in a periodic multilayer structure consisting of superconducting and dielectric materials have also been reported [4–8]. Such a superconducting planar Bragg reflector (SPBR) has some basic distinctions compared to an all-dielectric plane Bragg reflector. For example, there exists a low-frequency PBG due to the combined effects of periodicity and of incorporating superconducting materials [5–7]. This low-frequency PBG is further tunable as a function of the temperature and the applied static magnetic field as well. This tunable feature comes from the temperature- and field-dependent penetration length of a superconductor. Moreover, in the region near the threshold frequency of the bulk superconductor, which plays a similar role as the plasma frequency in metal, some extraordinary optical properties in an SPBR can be seen [9].

A Bragg reflector with an annular geometric structure shown in Fig. 1 has now been realized with the advance of modern fabrication techniques. By creating a ring defect into the annular periodic multilayer structure, an annular resonator or laser has been recently reported [10,11]. Such an annular laser has a very important feature of vertical emission which makes it of particular use in optical electronics and communication. Motivated by these facts, in this paper, instead of the SPBR, we shall theoretically investigate the optical reflection properties of a superconducting annular Bragg reflector (SABR). In our analysis we use the two-fluid model for the superconductor [12,13] together with the transfer matrix method for the cylindrical waves developed by Kaliteevski et al. [14]. With the fact that the field solutions of the cylindrical waves are closely related to the azimuthal mode number, denoted by m, for both the TE and TM waves, optical properties at different m-numbers will be examined. In this paper, we have found that an additional high-reflectance band or some reflection dips near the threshold wavelength of a superconductor can be found for the TM wave at an azimuthal mode number $m \geq 1$. These two distinct features behave like the localized passbands, which provide a feasible way of designing a narrowband transmission filter or an annular resonator without physically introducing any defect layer to break the periodicity of the structure. First we demonstrate that

* Corresponding author. Tel.: +886 2 29338260; fax: +886 2 86631954
E-mail addresses: jasperwu@ntnu.edu.tw (C.-J. Wu), yangtjr@yahoo.com.tw (T.-J. Yang).

0038-1098/$ – see front matter © 2009 Elsevier Ltd. All rights reserved.
doi:10.1016/j.ssc.2009.08.002

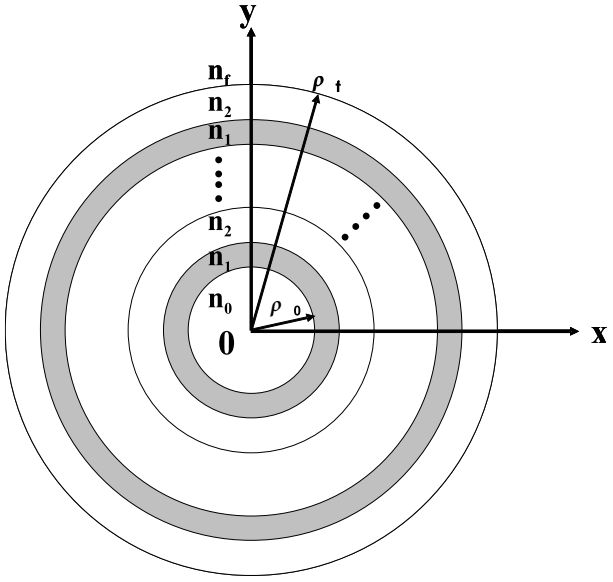

Fig. 1. The cross sectional view of an SABR, in which the constituent layers are 1 and 2 with refractive indices n_1 and n_2, respectively. The superconductor is layer 1 and layer 2 is the dielectric.

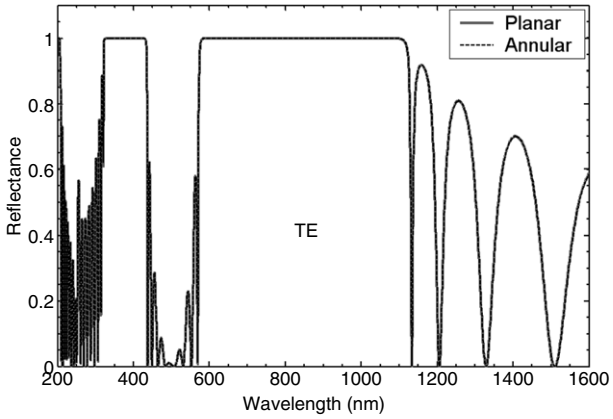

Fig. 2. Calculated wavelength-dependent reflectance for YBCO/MgO BRs., where the solid curve is for the SPBR, and the dashed curve is for the SABR.

the wavelength-dependent reflectance at $m = 0$ is nearly identical to that of the planar one-dimensional superconducting BR. Second, the reflectance spectra for the TM wave are plotted and compared at different values of m. Finally, the role played by the starting radius ρ_0 in this SABR will be illustrated.

2. Theory

The structure of an SABR is shown in Fig. 1, in which the inner core region has a refractive index of n_0 and a starting radius of ρ_0, the layer 1 with index n_1 is assumed to be the superconductor, and layer 2 having index n_2 is the dielectric layer. In addition, the index of refraction of the outer region is denoted by n_f. To calculate the reflectance at the first circular boundary, $\rho = \rho_0$, we use the transfer matrix method in the cylindrical waves [14]. The cylindrical wave is assumed to be diverging from the axis of symmetry, $\rho = 0$, and then impinges normally on the first circular interface of $\rho = \rho_0$.

Assuming an $\exp(j\omega t)$ time dependence for the electromagnetic fields, the source-free two curl Maxwell's equations are given by

$$\nabla \times E = -j\omega\mu H, \tag{1}$$

$$\nabla \times H = j\omega\varepsilon E. \tag{2}$$

In the circular cylindrical coordinates there are two possible modes, i.e., TE and TM modes. For TE wave, the nonzero fields, E_z, H_ϕ, and H_ρ in each single layer satisfy the following three equations,

$$\frac{1}{\rho}\frac{\partial E_z}{\partial \phi} = -j\omega\mu H_\rho, \tag{3a}$$

$$\frac{\partial E_z}{\partial \rho} = j\omega\mu H_\phi, \tag{3b}$$

$$\frac{\partial\left(\rho H_\phi\right)}{\partial \rho} - \frac{\partial H_\rho}{\partial \phi} = j\omega\varepsilon\rho E_z. \tag{3c}$$

With Eq. (3), the governing equation for tangential electric field E_z is given by

$$\rho\frac{\partial}{\partial\rho}\left(\rho\frac{\partial E_z}{\partial\rho}\right) - \rho^2\frac{1}{\mu}\frac{\partial\mu}{\partial\rho}\frac{\partial E_z}{\partial\rho} + \frac{\partial}{\partial\phi}\left(\frac{\partial E_z}{\partial\phi}\right) + \omega^2\mu\varepsilon\rho^2 E_z = 0. \tag{4}$$

The solution of Eq. (4) can be obtained by the method of separation of variables, with the result

$$E_z(\rho,\phi) = V(\rho)\,\Phi(\phi) = \left[AJ_m(k\rho) + BY_m(k\rho)\right]e^{jm\phi}, \tag{5}$$

where m is the azimuthal number and the radial part $V(\rho)$ satisfies the Bessel differential equation and therefore solution is written in Eq. (5). Here A and B are constants, $k = \omega\sqrt{\mu\varepsilon}$ is the wave number in the layer, J_m is a Bessel function, and Y_m is a Neumann function. Then according to Eq. (3b), the azimuthal part of magnetic field is given by

$$H_\phi(\rho,\phi) = U(\rho)\,\Phi(\phi) = -jp\left[AJ'_m(k\rho) + BY'_m(k\rho)\right]e^{jm\phi}, \tag{6}$$

where $p = \sqrt{\varepsilon/\mu}$ is the intrinsic admittance of the layer. Eqs. (5) and (6) enable us to construct a single layer matrix relating the electric and magnetic fields at its two interfaces. For instance, the matrix for the first layer (with refractive index n_1 and interfaces at $\rho = \rho_0$ and ρ_1) is written as [14]

$$\begin{bmatrix} V(\rho_1) \\ U(\rho_1) \end{bmatrix} = \mathbf{M}_1 \begin{bmatrix} V(\rho_0) \\ U(\rho_0) \end{bmatrix}, \tag{7}$$

where the single layer matrix

$$\mathbf{M}_1 = \begin{bmatrix} m_{11} & m_{12} \\ m_{21} & m_{22} \end{bmatrix},$$

has the following matrix elements

$$\begin{aligned} m_{11} &= \frac{\pi}{2}k_1\rho_0\left[Y'_m(k_1\rho_0)J_m(k_1\rho_1) - J'_m(k_1\rho_0)Y_m(k_1\rho_1)\right], \\ m_{12} &= j\frac{\pi}{2}\frac{k_1}{p_1}\rho_0\left[J_m(k_1\rho_0)Y_m(k_1\rho_1) - Y_m(k_1\rho_0)J_m(k_1\rho_1)\right], \\ m_{21} &= -j\frac{\pi}{2}k_1\rho_0 p_1\left[Y'_m(k_1\rho_0)J'_m(k_1\rho_1) - J'_m(k_1\rho_0)Y'_m(k_1\rho_1)\right], \\ m_{22} &= \frac{\pi}{2}k_1\rho_0\left[J_m(k_1\rho_0)Y'_m(k_1\rho_1) - Y_m(k_1\rho_0)J'_m(k_1\rho_1)\right], \end{aligned} \tag{8}$$

where $p_1 = \sqrt{\varepsilon_1/\mu_1}$. Obviously, the matrix elements are dependent on the radii of the two interfaces. Similarly, for ith layer the matrix can be obtained by some simple replacements, i.e., $\rho_0 \to \rho_{i-1}$, $\rho_1 \to \rho_i$, $k_1 \to k_i = \omega\sqrt{\mu_i\varepsilon_i}$, and $p_1 \to p_i = \sqrt{\varepsilon_i/\mu_i}$. In addition, with structure being periodic, one has $\varepsilon_i = \varepsilon_1$ if i = odd, and $\varepsilon_i = \varepsilon_2$ if i = even. For an N-period bilayer periodic reflector we have, in total, $2N$ layers and therefore there should be $2N$ matrices in order to set up the total system matrix $\mathbf{M}$ that relates the first and final interfaces as

$$\begin{bmatrix} V(\rho_f) \\ U(\rho_f) \end{bmatrix} = \mathbf{M} \begin{bmatrix} V(\rho_0) \\ U(\rho_0) \end{bmatrix}, \tag{9}$$

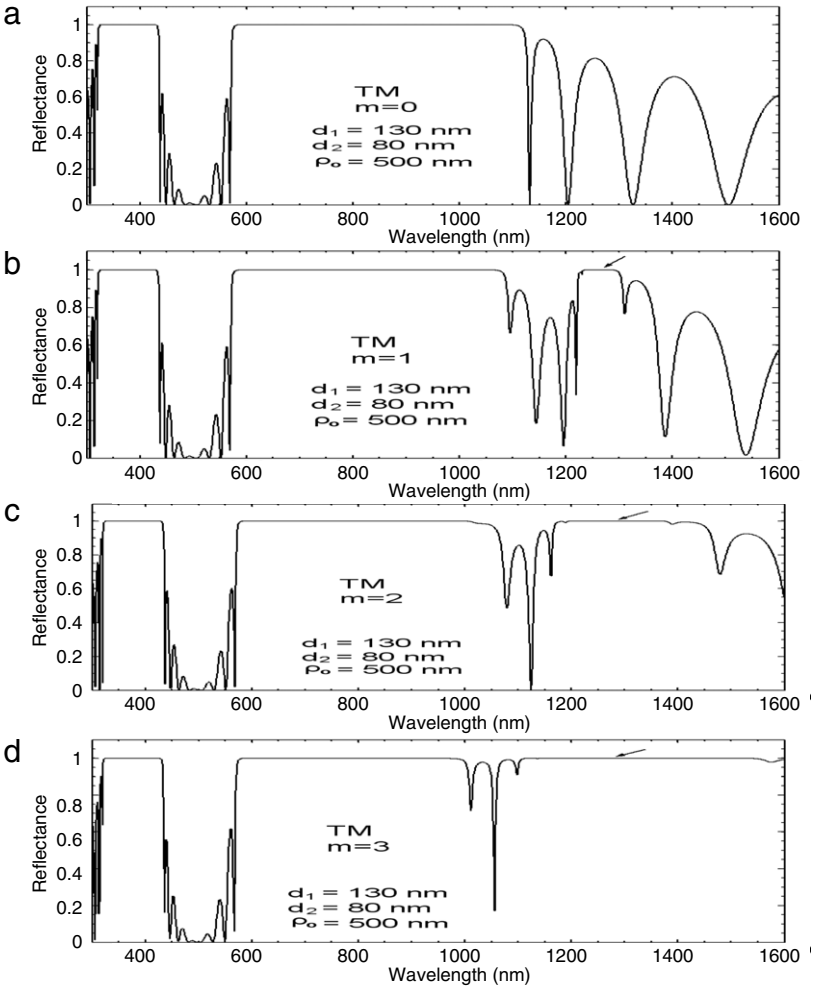

Fig. 3. Calculated reflectance spectra of TM wave at different azimuthal mode numbers, (a) $m = 0$, (b) $m = 1$, (c) $m = 2$ and (d) $m = 3$, respectively, under the conditions of $d_1 = 130$ nm, $d_2 = 80$ nm, $\rho_0 = 500$ nm and $N = 9$.

where

$$\mathbf{M} = \begin{bmatrix} M_{11} & M_{12} \\ M_{21} & M_{22} \end{bmatrix} = \mathbf{M}_{2N} \cdots \mathbf{M}_2 \mathbf{M}_1. \tag{10}$$

Unlike usual planar 1DPC, the analytic expressions for the matrix elements of **M** for an annular BR cannot be obtained because the elements of each single layer matrix are functions of the radii of the two interfaces. It thus has to be numerically calculated. With the calculated matrix elements, the reflection and transmission coefficients can be determined through the relationships given in Box I [14], where $p_0 = \sqrt{\varepsilon_0/\mu_0}$ and $p_f = \sqrt{\varepsilon_f/\mu_f}$ are the admittances of the starting and the last medium for the incident wave, M'_{11}, M'_{12}, M'_{21} and M'_{22} are the matrix elements of the inverse matrix of **M**, $K = \omega\sqrt{\mu_0\varepsilon_0}$ is the free-space wave number, and

$$C_{ml}^{(1,2)} = \frac{H_m^{(1,2)\prime}(k_l\rho_l)}{H_m^{(1,2)}(k_l\rho_l)}, \quad l = 0, f. \tag{11}$$

where $H_m^{(1)}$ and $H_m^{(2)}$ are the Hankel function of the first and second kind. The results for TM wave are also obtainable by simply replacing $\varepsilon \leftrightarrow \mu$, and $j \leftrightarrow -j$ in the formulas of TE wave.

Regarding the permittivity of the superconducting layer, we shall adopt the two-fluid model. According to the two-fluid this model the conductivity of a lossless superconductor is expressed as [5,6]

$$\sigma = -j\frac{1}{\omega\mu_0\lambda_L^2}, \tag{12}$$

where the temperature-dependent London penetration depth is given by

$$\lambda_L(T) = \frac{\lambda_0}{\sqrt{1 - \left(\frac{T}{T_c}\right)^4}}, \tag{13}$$

where λ_0 is the penetration depth at 0 K, and T_c is the critical temperature for the superconductor. The condition of a lossless superconductor is well described in Ref. [5]. With Eq. (12), the relative permittivity and the associated refractive index can be obtained and are given by

$$\varepsilon_{1r} = 1 - \frac{c^2}{\omega^2\lambda_L^2}, \tag{14}$$

$$n_1 = \sqrt{\varepsilon_{1r}} = \sqrt{1 - \frac{c^2}{\omega^2\lambda_L^2}}. \tag{15}$$

It is seen, from Eq. (15), that there is a threshold wavelength $\lambda_{th} = 2\pi\lambda_L$ at which n_1 is equal to zero. The threshold frequency, or the threshold wavelength, similar to the plasma frequency in metal characterizes the electromagnetic wave properties of a bulk superconductor.

$$r_d = \frac{\left(M'_{21} + jp_0 C^{(2)}_{m0} M'_{11}\right) - jp_f C^{(2)}_{mf}\left(M'_{22} + jp_0 C^{(2)}_{m0} M'_{12}\right)}{\left(-jp_0 C^{(1)}_{m0} M'_{11} - M'_{21}\right) - jp_f C^{(2)}_{mf}\left(-jp_0 C^{(1)}_{m0} M'_{12} - M'_{22}\right)},$$

$$t_d = \frac{4\sqrt{\varepsilon_0/\mu_0}}{\pi K \rho_0 H^{(2)}_m(k_0\rho_0) H^{(1)}_m(k_0\rho_0)\left[\left(-jp_0 C^{(1)}_{m0} M'_{11} - M'_{21}\right) - jp_f C^{(2)}_{mf}\left(-jp_0 C^{(1)}_{m0} M'_{12} - M'_{22}\right)\right]},$$

Box I.

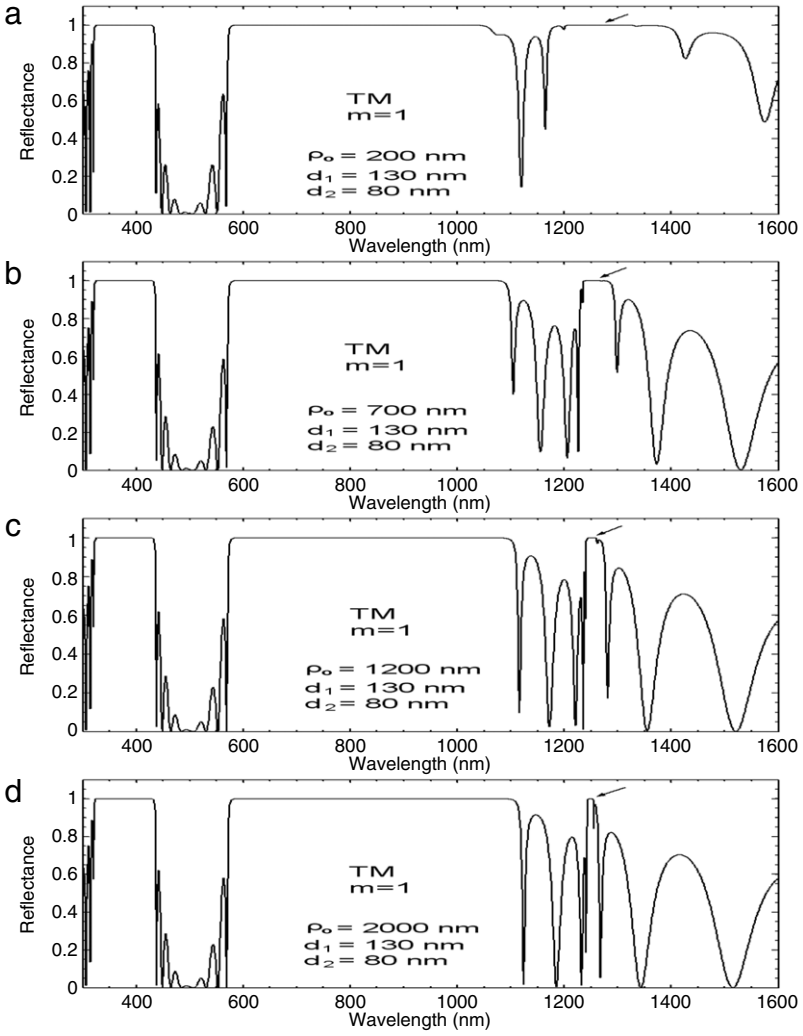

Fig. 4. Calculated reflectance spectra of TM wave at $m = 1$ for different starting radii (a) $\rho_0 = 200$ nm, (b) $\rho_0 = 700$ nm, (c) $\rho_0 = 1200$ nm and (d) $\rho_0 = 2000$ nm, respectively, under the conditions of $d_1 = 130$ nm, $d_2 = 80$ nm and $N = 9$.

3. Numerical results and discussion

To calculate the reflection response, the layer 1 is taken to be the typical high-T_c superconductor, $YBa_2Cu_3O_7$ (YBCO) with $T_c = 92$ K and $\lambda_0 = 140$ nm [15], and the layer 2 is MgO with $\varepsilon_{2r} = 10$. The operating temperature is $T = 77$ K in our simulation. The penetration depth λ_L and the permittivity ε_{1r} of YBCO can be calculated according to Eqs. (14) and (15). With these material parameters, the threshold wavelength of YBCO is calculated to be $\lambda_{th} = 1245$ nm. In addition, the SABR is immersed in free space, i.e, $n_0 = n_f = 1$. The thicknesses of YBCO and MgO layers are set to be $d_1 = 130$ nm and $d_2 = 80$ nm, respectively, and the number of periods is $N = 9$.

In Fig. 2, we plot the wavelength-dependent reflectance for both the SABR and SPBR in TE wave, where the dashed curve is for SABR with $\rho_0 = 1000$ nm at the lowest mode, $m = 0$, and the solid curve is for SPBR. It is seen that both of the reflection spectra almost coincide. This indicates that means the effect of the curved interfaces in an SABR at $m = 0$ can be neglected compared to the SPBR. In addition, there are two high-reflection bands (PBGs) in Fig. 2. The larger bandwidth covering the range from the orange light to the near infrared has the two bandedges of 598 nm and 1059 nm (bandwidth $\Delta\lambda = 461$ nm). The small bandwidth falling from the violet to the ultraviolet (UV) has two bandedges, 329 nm and 421 nm, and a bandwidth of $\Delta\lambda = 92$ nm. We can see that the $\lambda_{th} = 1245$ nm is not located within these two PBGs in this case.

Let us now investigate the reflectance at various values of m-number. Fig. 3 depict the TM-reflectance at $m = 0$ (a), 1 (b), 2 (c), and 3 (d), respectively, under the conditions of $d_1 = 130$ nm, $d_2 = 80$ nm, $\rho_0 = 500$ nm and $N = 9$. It is of interest to see that

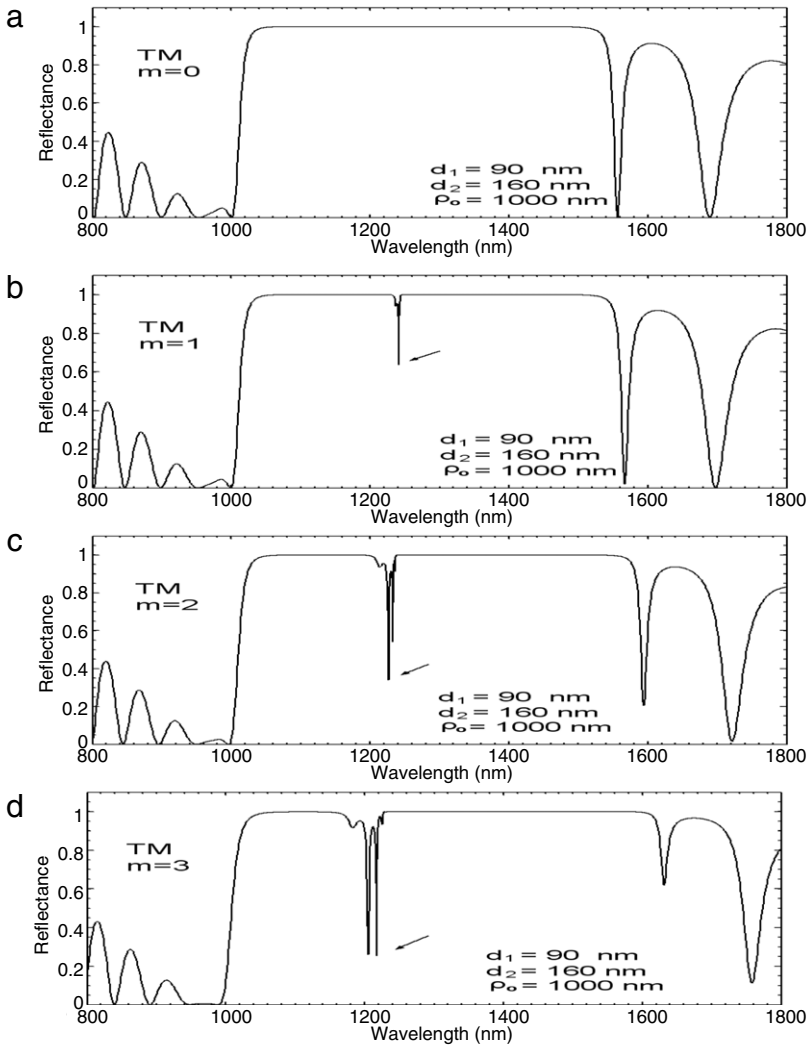

Fig. 5. Calculated reflectance spectra of TM wave for different azimuthal mode numbers (a) $m = 0$, (b) $m = 1$, (c) $m = 2$ and (d) $m = 3$, respectively, under the conditions of $d_1 = 90$ nm, $d_2 = 160$ nm, $\rho_0 = 1000$ nm and $N = 9$.

at $m \geq 1$ there is an additional PBG within which the threshold wavelength is contained. Such a PBG is referred to as a near-zero-n gap because within this gap the refractive index of a superconductor is much less than one and very close to zero. This gap is strongly dependent on the m-value, increasing largely as the m-value increases. This additional PBG however cannot be seen for the TE wave. This gap is due to the existence of radial component of the electric field, E_ρ. This E_ρ interacts with the superelectrons in the superconductor and thus a superpolariton gap is created. It is noted that this superpolariton gap seen only for the higher order azimuthal mode of the cylindrical wave has not been found in an SPBR in the TM wave. It also should be mentioned that here we do not present the results of TE wave because, in fact, at $m = 0$, the reflectance of TE wave is nearly identical to that of TM wave. Moreover, only a little distinction in reflectance at $m = 1$, 2, or 3 is seen when they are compared to that of at $m = 0$.

In Fig. 4, we plot TM-reflectance spectra of the SABR at four different starting radii, 200, 700, 1200, and 2000 nm at $m = 1$. It is seen that the size of superpolariton gap is strongly affected by ρ_0. The size apparently decreases as ρ_0 increases. That is, a narrowband gap could be obtained at a larger ρ_0. This feature suggests that we can control the superpolariton gap size by simply changing the starting radius. However, other PBGs are not changed pronouncedly as a function of the starting radius.

Finally, we shall investigate the PBG at which the threshold wavelength of the superconductor is located within it. To reach this end, we have chosen $d_1 = 90$ nm, $d_2 = 160$ nm, and $\rho_0 = 1000$ nm, and the TM-reflectance is plotted in Fig. 5. It is seen from Fig. 5(a) that the threshold wavelength $\lambda_{th} = 1245$ nm indeed falls within the PBG at $m = 0$. It is of interest to observe that, at $m \geq 1$, a sharp dip is seen in the vicinity of λ_{th}, as shown in Fig. 5(b)–(d). In addition to the enhancement of the dip due to the higher mode number, the number of dips is also increased. This phenomenon only arising from the higher order azimuthal mode of the cylindrical wave is not present in the SPBR in the normal incidence case, but similar dip(s) can be found in the oblique incidence in the TM wave [9]. The existence of such dips possibly enables us to design a circular transmission narrowband filter or resonator without introducing any physical defect. Moreover, a multi-resonance filter is also possible because of the presence of the multiple resonant dips. All these peculiar features are, in fact, not observed in a usual all-dielectric annular BR.

4. Summary

The photonic band structures of an SABR have been analyzed in this paper. At $m = 0$, the reflectance characteristics of an SABR is similar to that of an SPBR. At $m \geq 1$, we find that there is an additional PBG called the superpolariton gap only for the TM wave. We also find that there exist some dips when the wavelength of interest is near the threshold wavelength λ_{th} of a superconductor. Both these results are closely related to the higher order azimuthal

mode of the cylindrical wave in an SABR, which has not been seen in the SPBR. These special features make it possible for the SABR to be used for designing a narrowband transmission filter without inserting any physical defect layer in the structure.

Acknowledgements

The authors acknowledge the financial support from the National Science Council of the Republic of China (Taiwan) under grant Nos. NSC-97-2112-M-003-013-MY3 (C.-J. Wu), and NSC-97-2112-M-216-001 (T.-J. Yang).

References

[1] Y. Fink, J.N. Winn, S. Fan, C. Chen, J. Michel, J.D. Joannopoulos, E.L. Thomas, Science 282 (1998) 1679.
[2] A.V. Andreev, A.V. Balakin, I.A. Ozheredov, A.P. Shkurinov, Phys. Rev. E (2001) 016602.
[3] I.V. Shadrivov, A.A. Sukhorukov, Y.S. Kivshar, Phys. Rev. Lett. 95 (2005) 193903.
[4] H. Takeda, K. Yoshino, A.A. Zakhidov, Phys. Rev. B 70 (2004) 085109.
[5] C.H. Raymond Ooi, T.C. Au Yeung, Phys. Lett. A 259 (1999) 413.
[6] C.H. Raymond Ooi, T.C. Au Yeung, C.H. Kam, T.K. Lim, Phys. Rev. B 61 (2000) 5920.
[7] C.-J. Wu, M.-S. Chen, T.-J. Yang, Physica C 432 (2005) 133.
[8] O.L. Berman, Y.E. Lozovik, S.L. Eiderman, R.D. Coalson, Phys. Rev. B 74 (2006) 092505.
[9] Arafa H. Aly, H.-T. Hsu, T.-J. Yang, C.-J. Wu, C.K. Hwangbo, J. Appl. Phys. 105 (2009) 083917.
[10] J. Scheuer, W.M.J. Green, G. DeRose, A. Yariv, Opt. Lett. 29 (2004) 2641.
[11] William M.J. Green, J. Scheuer, G. DeRose, A. Yariv, Appl. Phys. Lett. 85 (2004) 3669.
[12] Michael Tinkham, Introduction to Superconductivity, 2nd ed., McGraw-Hill, New York, 1996.
[13] T. van Duzer, C.W. Turner, Principles of Superconductive Devices and Circuits, Edward Arnold, London, 1981.
[14] M.A. Kaliteevski, R.A. Abram, V.V. Nikolaev, G.S. Sokolovski, J. Mod. Opt. 46 (1999) 875.
[15] C.P. Poole Jr., H.A. Farach, R.J. Creswick, Superconductivity, Academic Press, San Diego, 1995.